# A Model of Air-Sea Flux of Carbon Dioxide in Response to Tropical Dynamics

Candidate Number: 341065
Supervisor: Dr L. Zanna
Word Count : 4811

April 27, 2014

**Abstract**

I propose a low order model to describe the carbon dioxide flux in the equatorial Pacific in response to the El Nino Southern Oscillation. The model assumes one contribution due to the temperature of the water and the wind speed at the surface of the ocean, and a second contribution due to water from the deep ocean being drawn up to the surface. Using this approach combined with a dynamical model, I am able to construct a solution which agrees well with observation on the magnitude of the flux, the difference in flux between the east and the west of the ocean and the inter-annual variation in flux. The model is not however able to capture the North, South variation in flux in this area of the ocean, probably as the model ignores advective currents.

## 1 Introduction

In this project, I aim to construct a simple model to describe the flux of carbon dioxide between the ocean and the atmosphere in the equatorial Pacific. In particular I aim to investigate how the $CO_2$ flux is affected by the El Nino Southern Oscillation (hereafter ENSO).

An El Nino event is when there is anomalously warm water in the equatorial Pacific for an extended period of time, typically several months. The temperature anomaly is usually strongest in the east or the centre of the Pacific basin. The corresponding event with colder than average water is named La Nina. ENSO is the term given to the irregular cycle of El Nino and La Nina event, and has a time period of between 2 and 7 years [1]

The following idealised model of the processes which dominate the dynamics in the equatorial Pacific help to explain why ENSO occurs.

Throughout this report, the ocean is considered to be a two layer ocean. This is a simple model in which the ocean is described as having two distinct layers, an upper, mixed layer, and a lower, deep ocean. For a given point in space and time, each layer is considered to constant properties over its entire depth. Only the mixed layer is able to interact with the atmosphere, and the properties of the deep ocean change only very slowly. On the time period of interest (the time period of ENSO of a few years) we take the properties of the deep ocean to be constant.

Under normal conditions, (neither El Nino nor La Nina) the easterly trade winds create a mean westerly flow in the water at the surface of the ocean. In the east of the basin, this causes water from the deep ocean to be drawn to the surface to replace the water moving to the west. I shall refer to this process of deep ocean water being drawn up to the surface as upwelling. This upwelled water is much cooler, (as shown is Figure 1), resulting in a cooler sea surface temperature (hereafter SST) in the east of the basin than in the west. The effect of this upwelled water can be seen by looking at the depth of the thermocline along the equator. The thermocline is a layer in the ocean where the temperature of the water changes very rapidly with depth. In a two layer ocean, this corresponds to the surface which marks the boundary between the mixed layer and the deep ocean. Figure 3 shows that under normal conditions, the thermocline is much shallower in the East of the basin than in the West. During an El Nino event, the profile of the thermocline is much flatter, and is much deeper than before in the East, and so is linked to warmer than average SST

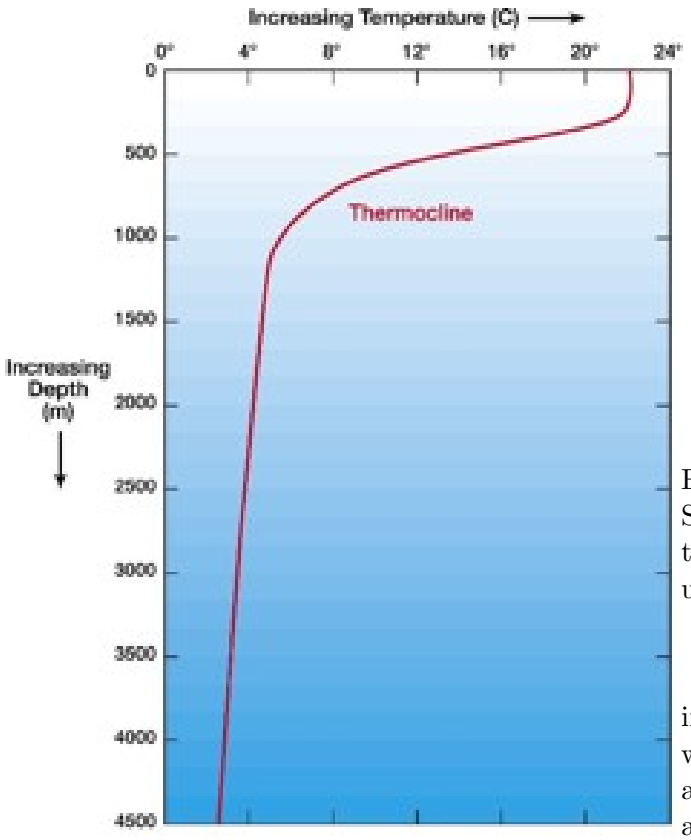


Figure 1: A typical low latitude ocean temperature profile with depth. Image from [2]

here. The reverse is true during a La Nina event, with a steeper profile indicating more upwelling in the East and so lower than average SST.

If the system is perturbed away from this mean state, for example by creating a positive SST anomaly in the centre of the Pacific, then we weaken the easterly trade winds (the Bjerkness hypothesis [4]). We expect that this will reduce the amount of water being upwelled in the East, and indeed it does excite a downwelling wave in the thermocline which will travel towards the East in the form of an equatorial Kelvin wave. At the same time, a westwards moving upwelling Rossby wave is created. We now have an El Nino event, with the thermocline deeper than normal in the East, and shallower than normal in the West. Eventually, the westwards moving Rossby waves will reach the western edge of the Pacific, and will be reflected as upwelling Kelvin waves which cancel the downwelling Kelvin waves and end the event. (Further knowledge of Kelvin and Rossby waves is not required here, except that they propagate with different, well known speeds).

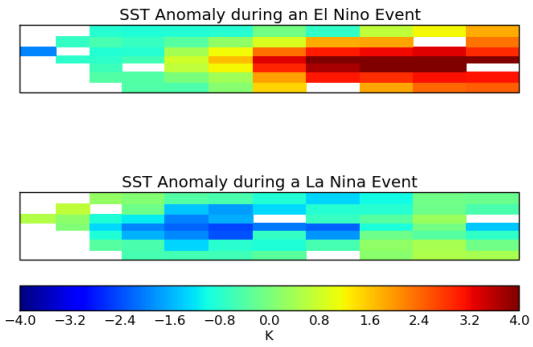


Figure 2: A comparison of the anomaly in Surface Sea Temperatures in the equatorial Pacific during the El Nino Event, La Nina events depicted in Figure 1. Data from [3]

ENSO is the largest observed source of variation in inter annual global SST, and as a result of this, we expect it to also have a large impact on the variability of the $CO_2$ flux between the ocean and the atmosphere. Understanding ENSO, and how it affects the exchange of $CO_2$ is therefore an important step in understanding how $CO_2$ is stored in the ocean. However, ENSO has proved to be a feature that is very difficult to model accurately, with the current climate models struggling to reproduce the correct combination of amplitude, location and power spectrum of ENSO. As a result, predictions of the carbon flux in this region are generally unreliable. Furthermore, due to the complex, numerical nature of these models, it is often difficult to gain any physical insight into the processes occurring.

In light of this, in this project I take a step back from these complex models, and instead attempt to build a low order, physically intuitive model of how the carbon flux varies during ENSO. The main goals of this project are therefore to create a model which is as simple as possible while still capturing the main effects, gives an answer which is easy to interpret physically, and is driven by observational data.

To do this, I begin by constructing a model of the carbon flux in terms of measurable quantities, and use observational data to test it. I then look to parametrise this model such that it depends on only one 'El Nino Strength' variable. Finally, I use this to provide an estimate of the carbon flux between the ocean and the atmosphere based on a model of

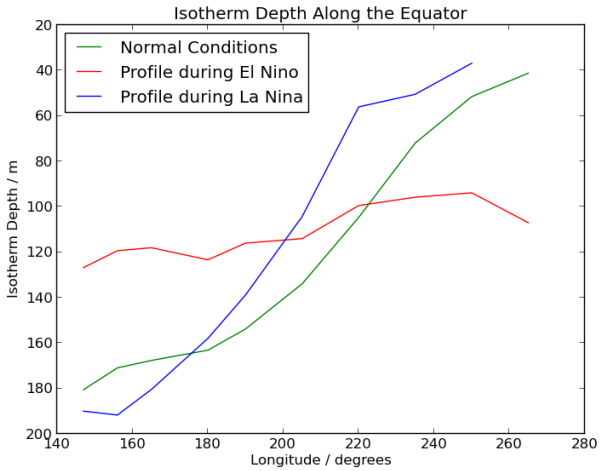


Figure 3: Comparison of the isotherm depth along the equator, showing the mean depth, (normal conditions), the depth during the El Nino event of 1998, and the depth during the La Nina event of 1999. It can clearly be seen that during the El Nino event, the thermocline is much flatter. Data from [3].

the El Nino Southern Oscillation.

## 2 Experimental Method

In constructing the model, I assume that the two factors which have largest effect on the carbon flux in this region are the surface temperature of the water, and the rate of upwelling. Two notable factors that I have chosen to ignore in simplifying the system are the biological life in the ocean and the horizontal advective currents. I also assume that it is possible to treat the flux due to the temperature of the water and the flux due to the upwelling as independent effects.

### 2.1 Flux due to SST

The SST is expected to have an effect on the amount of flux observed as both the solubility of a gas in water and the partial pressure of the gas depend on the temperature of the water. As the water heats up, the solubility decreases, the partial pressure increases, and so a more positive flux is expected at higher temperatures.

It is intuitive that the flux of carbon dioxide out of the water will be proportional to the difference in concentration of $CO_2$ between the ocean and the atmosphere, giving

$$F_{SST} = k \cdot \Delta[CO_2]. \tag{1}$$

The constant of proportionality here is the gas transfer velocity, and is typically take to be a function of the wind speed at the surface of the ocean only. We use the form suggested in [6] of;

$$k(v) = 87.6 \cdot (0.31v^2 - 0.71v + 7.76). \tag{2}$$

It is convenient to present the flux in units of $mol{\cdot}m^{-2}{\cdot}yr^{-1}$, requiring k in units of $m{\cdot}hour^{-1}$ and $\Delta[CO_2]$ in $mol \cdot m^{-3}$. (The factor of 87.6 in Equation 2 is due to a unit conversion from $cm \cdot hour^{-1}$.) From here, Henry's constant $H(T)$ is used, which relates for a given temperature, the concentration of gas in a liquid to its partial pressure via

$$H(T) = \frac{[CO_2]}{pCO_2}. \tag{3}$$

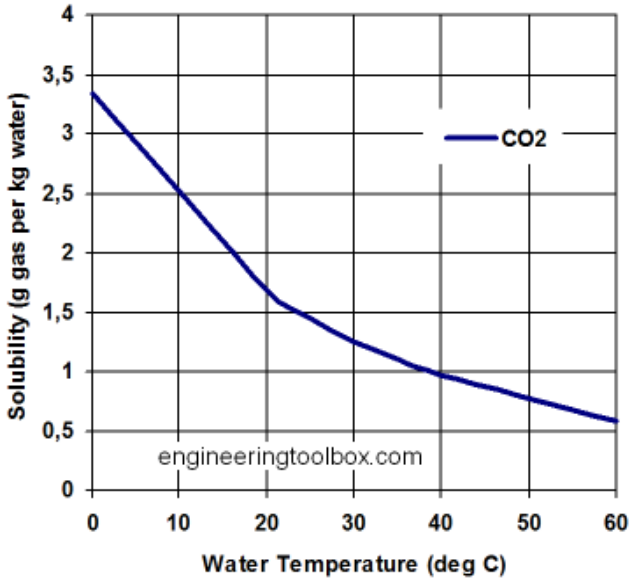


Figure 4: The solubility of carbon dioxide in water as a function of temperature. Image from [5]

$H(T)$ is a constant for a given temperature, so a value for it can be obtained by looking at a simple system with still water and gaseous $CO_2$ at a pressure of one atmosphere above it. The partial pressure is then one atmosphere (approximately the surface atmospheric pressure $P$) and the concentration of $CO_2$ in the water is then simply the solubility of the water at this temperature. The solubility of

$CO_2$ in water is shown in Figure 4, which motivates an approximation of the solubility in this temperature range as

$$S(t) = \frac{1000}{44} \cdot (22.4 - 0.07T). \quad (4)$$

(The numerical pre-factor is a unit conversion from $g \cdot kg^{-1}$ into $mol \cdot m^{-3}$ assuming a constant density of water of $1000 kgm^{-3}$.)

Combining Equations 3 and 4 gives

$$H(T) = \frac{1000 \cdot (22.4 - 0.07)}{44 \cdot P}. \quad (5)$$

Using Henry's constant, Equation 1 can be rewritten as

$$F_{SST} = H(T)k(v)\{pCO_2^{ocean} - pCO_2^{air}\}, \quad (6)$$

where $pCO_2$ is the partial pressure of $CO_2$. In order to progress further, I make use of the results of [7] to parametrise the $pCO_2$ as

$$pCO_2^{ocean} = Ae^{0.0423T}, \quad (7)$$

where $A$ is a parameter to be chosen later.

Finally, assuming a constant mole fraction of $CO_2$ in the atmosphere, $f$, gives

$$pCO_2^{air} = fP, \quad (8)$$

where $P$ here is the atmospheric pressure at the surface of the ocean.

This gives an carbon flux due to SST of the form

$$F_{SST} = Hk\{Ae^{0.0423T} - fP\} \quad (9)$$

## 2.2 Flux due to Upwelling

The upwelling is expected to have an effect on the $CO_2$ flux because the deep water is far cooler and richer in $CO_2$ than the water in the mixed layer (Figure 1). As this water is brought to the surface, it warms up, and releases some of the $CO_2$ contained within it.

The amount of $CO_2$ released per unit area in this process is roughly estimated as being equal to the amount of carbon dioxide released per unit volume multiplied by the upwelling velocity, $w$. The amount of carbon released per unit volume is calculated as the change in the concentration of $CO_2$, and I make the assumption that the deep ocean water is saturated for a partial pressure $fP$.

As before, the concentration is estimated as $[CO_2] = H \cdot pCO_2^{air}$ giving

$$[CO_2] = \frac{f \cdot 1000 \cdot (22.4 - 0.07T)}{44}, \quad (10)$$

which suggests a change in concentration of

$$\Delta[CO_2] = \frac{70 \cdot f \cdot \Delta T}{44}, \quad (11)$$

where $\Delta T$ is a parameter representing the change in temperature experienced by the water as it rises.

Finally, this results in a flux due to an upwelling velocity of $w$ of

$$F_{upwelling} = \frac{70 \cdot f \cdot \Delta T}{44}. \quad (12)$$

## 2.3 Whole Model

Adding the contribution from SST, (Equation 9), and the contribution from upwelling (Equation 12), gives the following equation for the total carbon flux

$$F_{total} = Hk \cdot \{Ae^{\alpha T} - fP\} + \frac{70 f \Delta T w}{44}. \quad (13)$$

## 2.4 Estimation of Upwelling Rate

Equation 13 serves as a clear and physically intuitive description of the processes assumed to drive the carbon flux, however, this form of the equation is difficult to use in practice as the upwelling rate $w$ is very small and so is almost never measured. This lack of data makes it necessary for us to construct a simple model to approximate the value of $w$ from variables for which data is more available.

The region of interest is a narrow strip close to the equator, and therefore all of the data is taken from points with very similar latitudes. Additionally, near the equator currents predominantly run along the equator rather than across it. These two factors motivate the assumption that if there was no upwelling anywhere in the basin, the temperature profile with depth should be identical anywhere in the basin. This is not what is observed, and so we make the approximation that the deviations are due to upwelling cold water.

A useful variable to use here is the heat content of the water per unit area (calculated as an integral of the heat content over the top $300m$ of the

ocean). The model of the dynamics in the Pacific basin presented in the introduction suggests that there should be very little upwelling in the west of the basin, and so I make the assumption that the heat content here is what we would expect to find in the absence of upwelling. This will be our reference heat content ($Heat_{ref}$). At all other points, a heat difference is then calculated, finding that the heat content is lower in the east of the basin. Figure 5 illustrates a rough method of converting this heat difference into an upwelling rate.

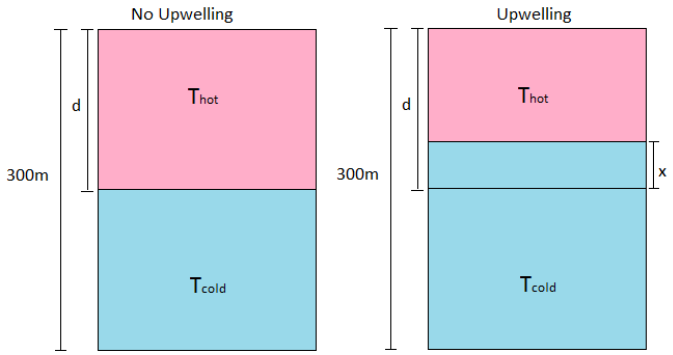


Figure 5: On the left is an idealised model of the west of the basin, where there is no upwelling. There are two layers in the ocean, with a depth $d$ of warm water, and the remainder of the $330m$ is colder, deep water. On the right, representing the east of the basin, where the heat content is lower, we attribute the heat difference to an extra depth $x$ of cold water.

$$\begin{aligned} Heat_{ref} &= \rho c d T_{hot} + \rho c (300-d) T_{cold} \\ Heat_{actual} &= \rho c (d-x) T_{hot} + \rho c (300-d+x) T_{cold} \\ \Delta Heat &= Heat_{ref} - Heat_{actual} \\ &= mcx\Delta T \end{aligned} \tag{14}$$

where $\rho$ is the density of water, $c$, is the specific heat capacity of water, and I have defined $\Delta T = T_{hot} - T_{cold}$.

Rearranging to find the extra depth of cold water $x$

$$x = \frac{\Delta Heat}{\rho c \Delta T} \tag{15}$$

In order to obtain an upwelling velocity from the additional depth of cold water, I introduce a parameter, $R$, the replenishment rate, which represents the frequency with which that depth of cold water is replaced.

From this, the upwelling rate, $w$, can be calculated as

$$w = \frac{R \cdot \Delta Heat}{\rho c \Delta T}. \tag{16}$$

## 2.5 Fitting Model Parameters to Data

Combining Equation 13 and Equation 16 produces a final estimate for the carbon flux.

$$F_{total} = Hk \cdot \{Ae^{0.0423T} - fP\} + \frac{70 f R \Delta Heat}{44 \rho c}. \tag{17}$$

Finally, values must be obtained for the model parameters.

- $f$: This is the mole fraction of $CO_2$ in the atmosphere. As the atmosphere is well mixed, $f$ is assumed to be a constant in space and time, and has a value of $3.8 \times 10^{-4}$ (atmospheric concentration of $CO_2$ is about 380ppm).
- $Heat_{ref}$: This is the expected heat content in the absence of upwelling. I selected the grid point (0N, 156W) to be the reference point, and allow for a seasonal cycle. The reference value will therefore be the average for that month of the year.
- $A$: This is chosen by picking a temperature and pressure for which the carbon flux due to SST is zero. By examining Figure 10, I select a region in the west of the equatorial Pacific as our zero point, and by looking at mean SST and surface pressure in this region, obtained a value of $1.085 \times 10^{-4}$.
- $R$: As there is no precise data for the upwelling velocity, this was chosen to be 5000 by tuning the model to best fit the observed flux. The corresponding value for $w$ peaks at about $5 \times 10^{-4} cms^{-1}$ (assuming a $\Delta T$ of $5K$).

## 2.6 Effect of ENSO on Carbon Flux

I would now like to use this model to calculate how the carbon flux varies with time during ENSO. In order to do this, it is necessary to relate the variables used in equation 17 to some parameter representing the strength of ENSO at that time. For

| Variable | PMCC | Gradient |
|---|---|---|
| SST | 0.89 | 0.053 |
| Heat Content | 0.97 | 0.0054 |
| Surface Pressure | -0.55 | -0.018 |
| Surface Wind Speed | 0.63 | 0.022 |

Table 1: The correlation coefficient and the gradient of the line of best fit for the scatter plots between the anomaly in the variables shown and the anomaly in 20C isotherm depth at (0N, 110W). (Surface Pressure refers to the atmospheric pressure at the surface of the ocean).

our purposes, we choose the thermocline depth as our ENSO parameter, as there is a large amount of data for this, and it is a common diagnostic to describe ENSO. It is a common practice (change wording here) to characterise all variables in terms of thermocline depth, (reference or change) and is convenient for us to take this approach.

For this paper, I use data taken from [3]. The TAO data is gathered from a system of buoys in the Pacific which cover a region from 8N to 8S, and from 137E to 110W. These buoys gather data daily, and records go back to about 1960, although gaps in the data are frequent, especially early in the time series. The data set does not include data for the thermocline depth as such, but does include data for the 20C isotherm depth, which we expect to be a surface within the thin thermocline layer, so we shall use this as a substitute. Due to the frequent gaps in the data, I first convert the data to a monthly mean, thus reducing the impact of individual missing days or weeks. I then calculate a mean value for each of the variables used (SST, heat content, surface air pressure, surface wind speed and 20C isotherm depth). It is important to be able to separate the effect of ENSO from the effect of the annual cycle, so I calculate a separate mean for each month of the year. From this, I am able to obtain a time series of the anomaly in each of the variables, calculated by subtracting the expected value for that month from the actual value recorded. A scatter plot of the anomaly in each of these variables against the 20C isotherm depth anomaly is then created, and the Pearson Product-Moment Correlation Coefficient is calculated along with a line of best fit. The results are shown in Table 1 and Figure 6.

There is a strong correlation between the SST and the isotherm depth, and an even better correlation

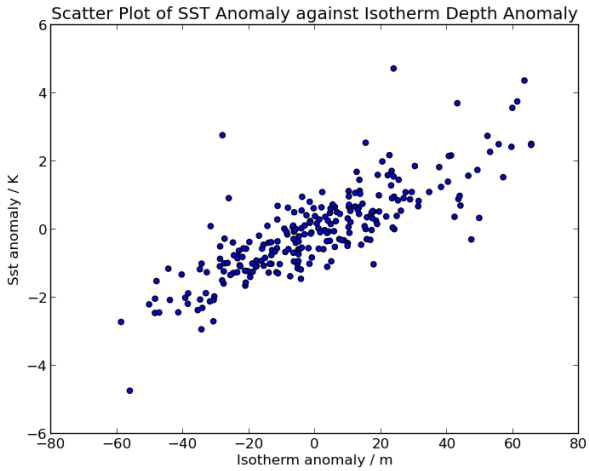


Figure 6: Scatter plot of the anomaly in SST against the anomaly in isotherm depth.

between the heat content and the isotherm depth. The correlations with pressure and wind speed were much weaker, but are still considered good enough to gain a rough parametrisation of them from the line of best fit and the monthly mean.

This provides a method of estimating a carbon flux using the thermocline depth as the only parameter.

## 2.7 A Simple Model of ENSO

We now wish to demonstrate our ability to generate a prediction of the carbon flux based on a dynamical model of ENSO. In this case, we shall use the simple model of ENSO proposed in [8]. This model is excellent for our purposes as it is one of the simplest which still exhibits the low order chaotic behaviour that we observe, has a time period which approximately agrees with observation, and shows seasonal locking. It also characterises ENSO in terms of the thermocline depth alone.

The model is based around the idea of a delayed oscillator. This uses the description of ENSO that we put forward in the introduction, where we have an eastwards propagating Kelvin wave, which reaches the east of the basin a time $\tau_1$ after being created. At this point,the coupling between the ocean and the atmosphere allows for this wave to have an impact on the centre of the basin via the wind. Along with the Kelvin wave, a westwards propagating Rossby wave is also created, and this is reflected off the western boundary of the basin

and then travels eastwards as a Kelvin wave. This wave eventually reaches the East of the basin at a time $\tau_2$ at which point it also has an effect on the anomaly at the centre of the basin.

By adding a seasonal cycle to this concept, it is possible to construct a simple equation for the rate of change of thermocline depth

$$\frac{dh}{dt} = aA[h(t-\tau_1)] - bA[h(t-\tau_2)] + c\cdot\cos(\omega t), \quad (18)$$

where $a$, $b$, and $c$ are parameters, and $A[h]$ is a function defining the coupling between the ocean and the atmosphere.

$\tau_1$ and $\tau_2$ can be easily calculated as the time taken for the waves to propagate the required distance;

$$\tau_1 = \frac{L}{2C_{Kelvin}} \quad (19)$$

$$\tau_2 = \frac{L}{2C_{Rossby}} + \frac{L}{C_{Kelvin}} \quad (20)$$

Here, $L$ is the width of the Pacific basin, and $C_{Kelvin}$ = and $C_{Rossby}$ = are the speeds of the Kelvin and Rossby waves respectively.

For the form of $A[h]$, I follow the suggestion of [9],

$$lookuphowtodothisagain!!! \quad (21)$$

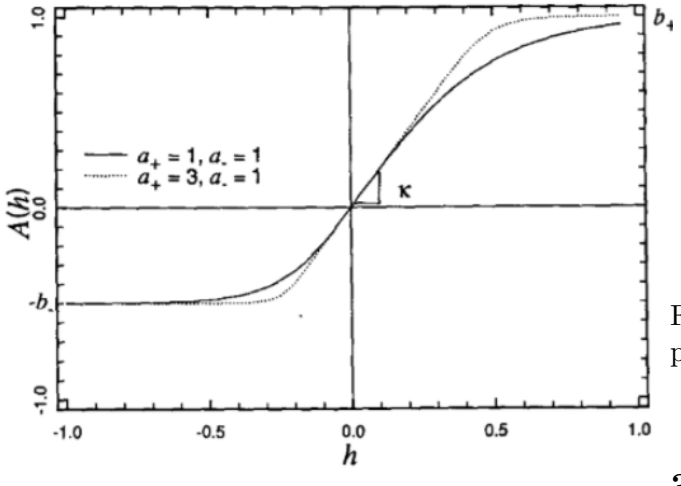


FIG. 2. Forcing function $A(h)$ given by Eq. (9).

Figure 7: Form of $A[h]$ given by Equation 21. Image from [9]

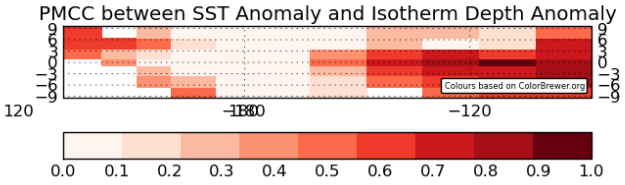


Figure 8: A plot of the correlation between SST and isotherm depth.

The predicted form of ENSO varies greatly depending on the choice of parameters. For a full discussion of how the parameters affect the model, see [8] and [9], for our purposes, the parameters are as in [8] with $\kappa = 2.0$. This choice of parameters gives the best possible mix of period of oscillation, seasonal locking, and chaotic behaviour. Figure 9 shows a plot of the time series of this model against the observed data.

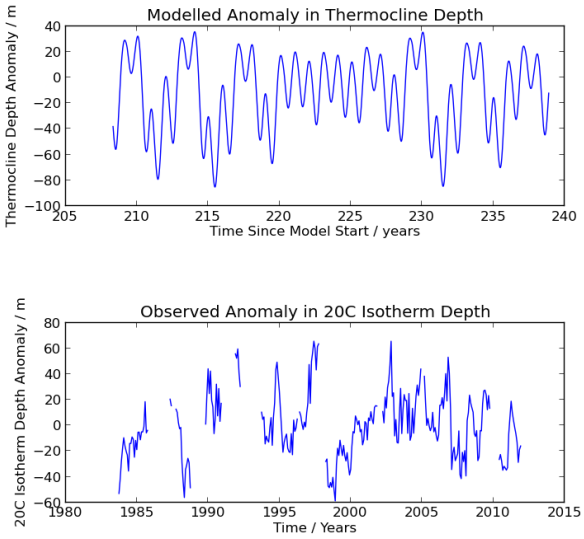


Figure 9: Comparison of the output of the parametrised model with the observational data.)

## 3 Results

Figure 10 shows the observed global carbon flux, which acts as the truth against which the model is tested. In Figure 11 I present a plot of the time averaged carbon flux over the whole of the basin, com-

paring observation with the output of the model. This plots is created using Equation 17 with observation data from [3] to create a carbon flux map for each month since 1960. We note that while there was sufficient data for SST, heat content, isotherm depth and wind speed, the data for pressure does not exist for many of the grid points. In order to preserve enough data points, we have made the assumption that pressure is a constant in time and space. This is not a terrible assumption as the variance in the surface pressure is small and so $\Delta pCO_2$ is dominated by the $pCO_2^{ocean}$ term. We set this constant to be 101kPa. The time average is calculated for each grid point as a mean of all of the months for which there is data. In all of the plots shown, we have defined a positive value to refer to a flux of carbon dioxide out of the ocean.

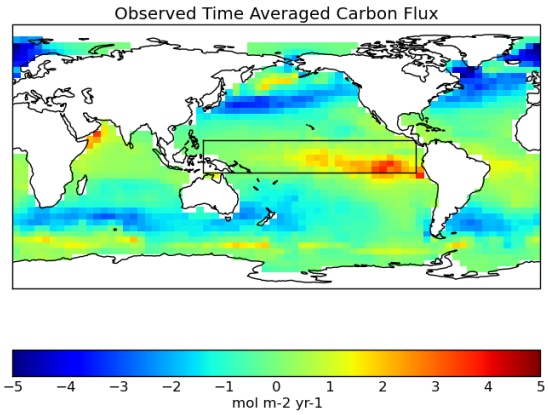


Figure 10: Observational time averaged carbon flux. Data from [3]. The highlighted box represents our region of interest for this project.

It is clear that the model predicts a much larger flux than expected in the North of the basin, but in the South of the basin, the prediction matches the observational data well. Figure 12 illustrates this by plotting the time averaged carbon flux along a slice through the data at a latitude of 4S.

In order to better examine how the carbon flux varies with time, I select a single grid point, in this case (0N, 110W), and plot the time series of the carbon flux at that point. I have chosen this grid point because there are stronger correlations between the variables in the east of the basin than in the west, and so many of our assumptions will be most reliable in this region. It is also a grid point in which the data is amongst the most complete, and allows for comparison with the flux based on the modelled thermocline anomaly, which is only valid for a point in the east of the basin. Figure 13 shows the plots for the carbon flux as a function of time.

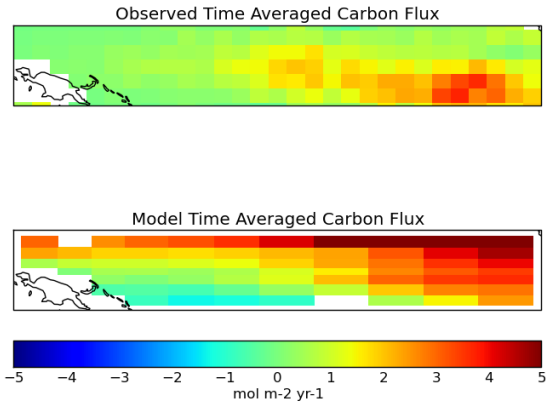


Figure 11: A comparison of the observed carbon flux and the carbon flux given by the model.

It is also possible to compare how to flux varies in different parts of the basin. Figure 14 compares the flux in the west of the basin to the flux in the east of the basin.

Finally, I aim to show that I am able to make a prediction of the carbon flux based on a model of how the thermocline depth evolves with time. In order to do this, all of the variables have been parametrised in terms of the isotherm depth anomaly. In order to test the validity of this approach, Figure 15 compares a plot of the carbon flux at (0N, 110W) when calculated using the data each of the variables, and when using the historic isotherm depth to parametrise all other variables.

We note the the variability in the parametrised model is much lower than in the unparametrised version, but that the mean values and the shape of the plots are similar. Proceeding with this method, we are now able to plot the predicted carbon flux based on the model of the thermocline anomaly. We have scaled the thermocline anomaly by a factor of 50 so that the magnitude of the fluctuations are in line with the observed values. Figure 12 shows the result of this.

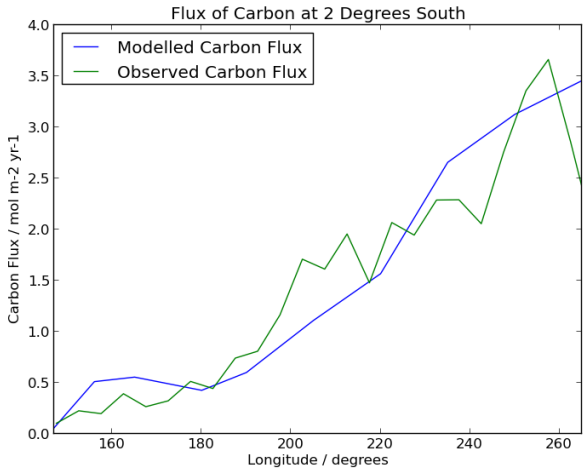


Figure 12: A comparison of the carbon flux across the basin at 4S shown in the data and predicted by the model.

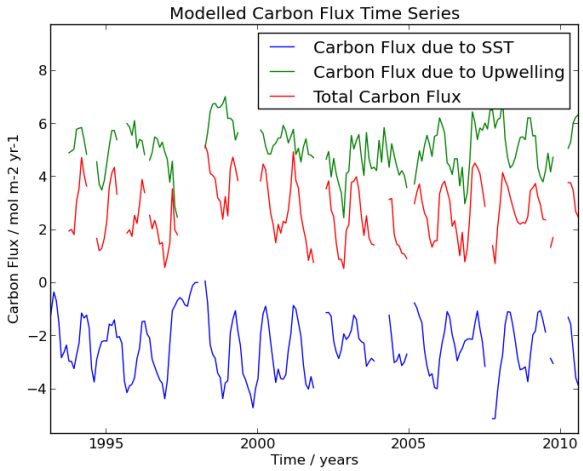


Figure 13: The carbon flux predicted by the model.

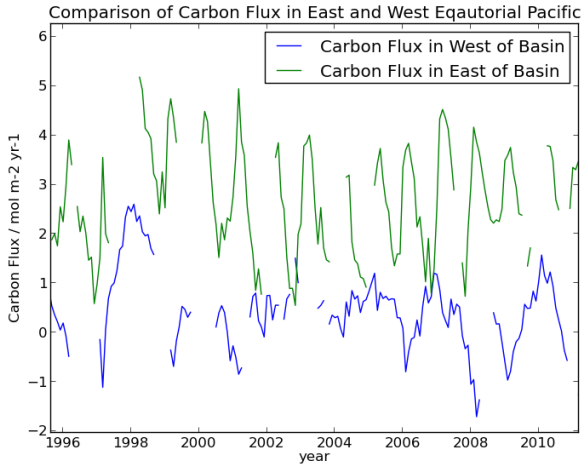


Figure 14: A comparison of the carbon flux in the east and west of the basin.

# 4 Analysis

In Figures 13 and 16, it is shown that our total flux in the East is comprised of a strongly positive flux due to the upwelling, and a slightly negative flux due to the SST. It is also clear that in general, the anomaly in $F_{SST}$ has the opposite sign to the anomaly in $F_{upwelling}$. This makes sense, as an increase in upwelling results in a decrease in the SST, however, it has an interesting effect on the inter-annual variation of the flux when comparing the parametrised and unparametrised variables (Figure 12). With this parametrised variables, the signs of $F_{SST}$ and $F_{upwelling}$ are always opposite, and so there is always a significant cancellation between them, making the variation in total flux smaller than the variation in either component. This is not true as much in the unparametrised version, where while the signs often opposed, this is not always the case, and the form of the components are not identical. The allows for a much larger variation in the flux.

When the inter-annual variability in the $CO_2$ flux that we obtain from our model is compared with observation, (reference) we find that our variation in the East of the basin roughly agrees with observation, both with a value of about 1 $molm^{-2}yr^{-1}$, but our variability in the West of the basin does not drop off as it does in the observed data. This could be due to the fact that the thermocline is so much deeper in this section of the ocean. This extra depth will mean that the properties of this region will be much slower to change, and could damp the effect of ENSO more than suggested in the model.

From Figure 12, we can see that the model captures the East, West pattern very well. Both the magnitude of the flux and the variation of the flux between the east and west of the ocean agree quite well with observation. This suggests that the proposed model is succeeding in capturing much of the observed behaviour and is an encouraging result. However, our model shows significant North-South gradient which does not agree with the data. A possible explanation of this is the ocean currents. Our weakest assumption appears to be in our estima-

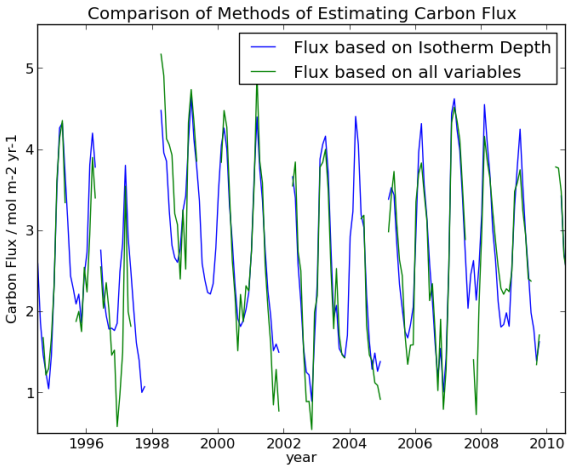


Figure 15: Time series of the carbon flux at (0N, 110W) based on (a) model with all variables from data and (b) all variables parametrised in terms of isotherm height.

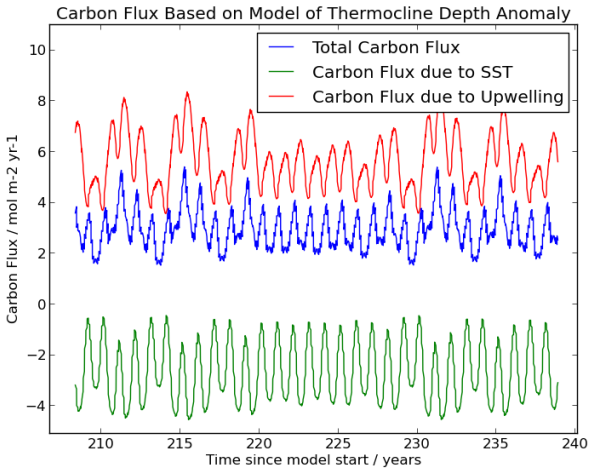


Figure 16: The flux at the grid point (0N, 110W) based on a model for the thermocline height. Plotted are lines representing the total carbon flux, the contribution due to SST,and the contribution due to the upwelling.

tion of the upwelling velocity, where we have had to attribute all of difference in heat to upwelling. In the North-East of the basin, this is not the case, as there is the additional effect of cooler water being brought down from North of the equator (Figure 17). As a result of this, the water in this region is cooler than elsewhere, and we have over estimated the upwelling rate, giving us the false result. In favour of this explanation, as about 4S, where Figure 14 indicates that the approximation of a purely westwards flow is best, we obtain the results which best match observation.

Another effect that we have ignored in this model is that of biology. We would expect that this would have the effect of decreasing the carbon flux, as the biological life has the net effect of absorbing $CO_2$ (reference) and carrying it down to the deep ocean when it dies. The impact of ignoring this effect is not as obvious in our results, and this is possibly because the amount of biological life is also correlated to the upwelling rate. This is because as well as being rich in $CO_2$, the deep ocean is also rich in other nutrients that help to sustain life. To a first approximation, it may well be reasonable to approximate the contribution from biology as being equal to $const + K_{bio}w$. If this is the case, then the impact of biology would only be to change the values of the parameters used. The *const* term would effect the value of $A$, and the $K_{bio}$ would effect the value of $R$.

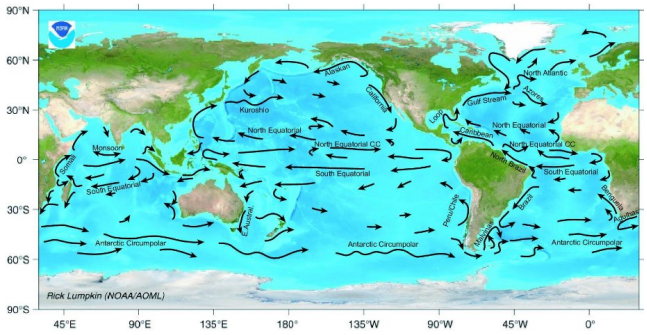


Figure 17: Map of the ocean surface currents. (reference)

This would suggest that our values for both $F_{SST}$ and $F_{upwelling}$ are slightly too low, and would be difficult to observe in the data. Alternately, the effect of biology could simply be very small in comparison to the other factors.

A third large assumption made in this model is in the estimation of the concentration of CO2 in the upwelling water. I currently assume that this water has a concentration equal to the saturation of water at this temperature in equilibrium with the atmosphere. However, water from the deep ocean interacts very little with the atmosphere, and so this is a poor assumption. A potential error in this calculation would result in an error in the amount of CO2 released per unit area per unit upwelling. As

the model is calibrated to give the correct carbon flux, this error would be likely to only effect the size of the replenishment rate $R$.

# 5 Conclusion

I have shown that it is possible to reproduce many of the features seen in the air-sea carbon dioxide flux in the equatorial Pacific by considering only the flux due to the temperature of the water and the flux due to the upwelling of water from the deep ocean. In particular, the model is able to produce a profile of the carbon flux along a given latitude which agrees well with observation. This result is especially strong for a latitude just south of the equator.

I was also to produce an estimate of the carbon flux based on a dynamical model of the thermocline depth. In order to achieve this, all of the variables are parametrised in terms of the thermocline depth. This approach is only valid in the east of the basin, where the correlations between the anomaly in thermocline depth is best correlated with the anomaly in the other variables, but we were able to show that within this limit, the approximation works well. One disadvantage of this method however, is that the inter-annual variation in the carbon flux is lower than when the raw data is used for all of the variables.

These successes suggest that the complex dynamics in the equatorial Pacific can be well represented by a process based, low order model. However, there are some features in the data which are not well represented by this model. Most notably, the model shows a clear north-south gradient in the carbon flux, which disagrees with observation. A possible explanation of this is that in the north-east of the basin, a current of cold water from the north is reducing the temperature of the water. In our model we have assumed that any cooling is due to upwelling, and so by ignoring this current, we have overestimated the amount of upwelling, and so overestimated the carbon flux.

The susceptibility of the model to ocean currents highlights that this model is likely only to be applicable in the equatorial Pacific. In addition to this, in other areas of the ocean there may be other dynamical effects which are not taken account of here. For example in many areas of the ocean, such as (place), there is downwelling water, which we are unable to model.

In this project, I have shown that a low order linear model captures enough of the dynamics in the equatorial Pacific to make further investigation interesting. The most obvious cause of error appears to be that I have ignored the horizontal advective currents. It would therefore be desirable to find a method of parametrising the effects of the currents. However, it is not clear how this could be easily achieved. Another factor that could be introduced given more time is the effect of biological life in the ocean. As discussed in the Analysis, while this would probably be possible given more time, it may not affect the end result significantly. Further, it would be interesting to examine the possibility of using this low order model in conjunction with a much more complex climate model, either to help analyse the output of the climate model, or to help increase the speed of the model by making use of some of the relationships discovered here.

# References


[1] The UK Met Office : El Nino, La Nina and the Southern Oscillation. Available at http://www.metoffice.gov.uk/research/climate/seasonal-to-decadal/gpc-outlooks/el-nino-la-nina/enso-d escription (Accessed 26 April 2014)

[2] Hurricanes: Science and Society. Available at http://www.hurricanescience.org/science/observation/ship (Accessed 26 April 2014)

[3] Tropical Ocean Atmosphere Project. Available at http://www.pmel.noaa.gov/tao/ (Accessed 30 March 2014)

[4] J. Bjerknes, Atmospheric Teleconnerctions from the Equatorial Pacific, *Monthly Weather Review*, **97**, 163-172 (1969).

[5] The Engineering Toolbox. Available at http://www.engineeringtoolbox.com/gases-solubility-water-d_1148.html. (Accessed 30 March 2014)

[6] C.D. Jeffery, I.S. Robinson, D.K. Woolf, Tuning a Physically Based Model of the Air-Sea Gas Transfer Velocity, *Ocean Modelling*, **31**, 28-35. (2009)

[7] T. Takahashi, Surface Variation of CO2 and Nutrients in the High Latitude Surface Oceans: A Comparative Study, *Global Biochemical Studies*, **7**, 843-878 (1993)

[8] E. Tziperman, L. Stone, M.A. Cane, H Jarosh, El Nino Chaos: Overlapping of Resonances Between the Seasonal Cycle and the Pacific Ocean Atmosphere Oscillator, *Science*, **264** 72-74 (1994)

[9] M. Munnich, M.A. Cane, S.E. Zebiak, A Study of Self-Excited Oscillations of the Tropical Ocean Atmosphere System. Part II: Nonlinear Cases. *J. Atmos. Sci.* **48**, 1238-1248 (1991)